9th ANKARA INTERNATIONAL AEROSPACE CONFERENCE **AIAC-2017-114**
20-22 September 2017 - METU, Ankara TURKEY

SHEAR-LAYER-ADAPTED DELAYED DETACHED-EDDY SIMULATION OF A TRANSONIC OPEN CAVITY FLOW

Özgür Yalçın*, Kenan Cengiz†, and Yusuf Özyörük‡
METU
Ankara, TURKEY

ABSTRACT

Open (deep) cavities in aerodynamic structures contain highly turbulent and acoustic flow fields because of the aft wall impingement of the shear-layer that separates from the upstream edge of the geometry. Although delayed detached-eddy simulation is a promising approach for massively separation regions, it could not capture the whole turbulent field due to its major drawback, the delay of transition to large-eddy simulation mode in the shear-layer. This study enhances the results around the separation region with the use of "shear-layer-adapted" length scale from literature which ensures the rapid transition from modeled to resolved mode of delayed detached-eddy simulation.

INTRODUCTION

Cavities at relatively high speeds, especially inside the fuselage of military aircraft carrying weapons, include a wide range of complex unsteady flow phenomena such as transition, separation, secondary corner flow, instability, and etc. According to the ratio of their length to depth, cavities are classified as shallow (closed), transitional, and open (deep) cavity. In shallow and transitional cavities flow separating from the upstream edge strikes the ceiling of the cavity, and then goes to the opposing edge. This causes a significant variation in pressure along the cavity yard, resulting in an unwanted pitching moment on the deployed missile or bomb. Instead, open cavities, where the separated flow strikes the aft wall directly, are preferred due to nearly uniform pressure distribution. However, in this case impinging flow directly on the downstream edge causes intense noise with distinct particular tones. The upstream propagating acoustic waves cause additional instability in the cavity flow forming a feedback mechanism which complicates the problem [Rossiter, 1964; Rockwell and Naudascher, 1978; Lawson and Barakos, 2011].

In literature, some computational studies showed that unsteady Reynolds-averaged Navier-Stokes (URANS) approach does not have a capability of resolving broadband spectrum in the cavities [Allen et al., 2005; Nayyar et al., 2005; Hamed et al., 2003]. URANS only could capture the main acoustic tones; not the high frequency components due to the inherent time averaging. On the other hand, although large-eddy simulation (LES) studies showed far better predictions of broadband spectrum

*GRA in a Department of Aerospace Engineering, Email: oyalcin@ae.metu.edu.tr
†GRA in a Department of Aerospace Engineering, Email: kcengiz@ae.metu.edu.tr
‡Prof. in a Department of Aerospace Engineering, Email: yusuf.ozyoruk@ae.metu.edu.tr

than URANS, LES application is expensive for high Reynolds number flow problems. Moreover, LES using scale invariance filtering could have difficulty to model subgrid scales near the aft corner regions where high vortical structures with relatively low Reynolds number exist [Gloerfelt et al., 2003; Lai and Luo, 2007; Larchevêque et al., 2004].

Studies using detached-eddy simulation (DES), which is a hybrid method of URANS and LES based on RANS equations, showed well-matched results with experimental studies, with accuracy levels similar to pure LES, but on much coarser grids due to RANS resolutions [Hamed et al., 2003; Kim et al., 2015; Nayyar et al., 2005; Luo and Xiao, 2015]. However, the major disadvantage of DES is the uncertain transition region between RANS and LES regions, called a gray area problem. This problem causes over/under prediction of acoustic tones although the trajectory of the whole spectrum could be captured. One of the main modifications to DES, called Delayed DES (DDES), solves the early activation issue of LES mode in URANS region with coarser grids. Despite the fact that this effort works well in many aerodynamic problems, it causes a delay of transition to turbulence in separated shear-layer and hence a delay of generation of 3D turbulent structures before the impingement in the cavity problems. This is the main reason of over/under prediction of sound spectra. Lately, "shear-layer-adapted" DDES (SLADDES) was introduced [Shur et al., 2015] to accelerate the transition to LES region in shear-layers. Although this improvement has been only recently implemented and tested successfully for some aerodynamic problems, we can claim that the implementation to cavity flows here in this paper is quite new to literature.

In the present work, a transonic flow with a Mach number of 0.85 and Reynolds number of 6.75×10^6 over an open but clean (without weapons or bombs) cavity geometry is simulated via the SLADDES approach. The simulation is carried out by the METUDES solver developed in the Middle East Technical University (METU) Aerospace Engineering Department [Cengiz and Özyörük, 2015]. In the remainder of the paper the features of the solver and the problem definition with the cavity geometry, mesh structure and boundary conditions are briefly given first, and then, the results of the turbulent flow field around the cavity domain are presented. Specifically, the behavior of separated shear-layer is analyzed. The velocity profiles at different locations are compared with those from an IDDES study [Luo and Xiao, 2015], and from a common benchmark LES study [Larchevêque et al., 2004] in details. The latter is a reliable source for comparisons since its results have shown quite well agreement with experiments. Finally, the "Conclusions" section highlights the key findings of the study.

METHOD

METUDES features

METUDES has been developed as an inhouse solver of the METU Aerospace Engineering Department. It is a time-accurate, compressible, Navier-Stokes (NS) solver, particularly designed for treating aeroacoustic problems. The code features a fourth-order low-dissipation low-dispersion finite volume spatial discretization [Kok, 2009] defined on 3D curvilinear grids. Low dissipation characteristic is based on symmetry-preserving scheme and low dispersion is based on dispersion-relation-preserving (DRP) optimization of the waves, both of which are crucial for resolution of wider range of sound sources and propagation of higher frequency sound waves simultaneously. The temporal discretization is the preconditioning-squared approach of [Turkel, 1997; Turkel and Vatsa, 2005] which makes use of dual-time stepping together with a low Mach number preconditioning and second order matrix time stepping. Moreover, a blended matrix dissipation suggested by [Potsdam et al., 2007] is added for properly scaled dissipation of spurious waves within the computational domain. METUDES simultaneously solves the RANS equations and the modified version of Spalart-Allmaras (SA) turbulence equation, as described below.

Crivellini's Modified Version of Spalart-Allmaras Turbulence Model:

The standard SA one equation model [Spalart and Allmaras, 1992] is applied as in the following non-conservation form and without the trip term:

$$\frac{\partial \tilde{\nu}}{\partial t} + \mathbf{V} \cdot \nabla \tilde{\nu} = \Psi + \Pi - \Phi \tag{1}$$

where $\mathbf{V}$ is the velocity vector of the flow field. Then, the turbulent eddy viscosity is obtained from;

$$\mu_{turb} = \rho f_{v1} \tilde{\nu} \tag{2}$$

The terms on the right hand side of Equation 1 represent diffusion, production, and destruction, respectively. They are computed as:

$$\begin{aligned} \Psi = \nabla \cdot \left(\frac{\nu + \tilde{\nu}}{\sigma} \nabla \tilde{\nu} \right), \quad \Pi = c_{b1}(1 - f_{t2}) \tilde{S} \tilde{\nu} + \frac{c_{b2}}{\sigma} |\nabla \tilde{\nu}|^2, \\ \Phi = (c_{w1} f_w - \frac{c_{b1}}{\kappa^2} f_{t2}) \left[\frac{\tilde{\nu}}{d} \right]^2 \end{aligned} \tag{3}$$

where ν is the molecular kinematic viscosity. All variables shown in these expressions are calculated as:

$$\begin{aligned} f_{v1} = \frac{\chi^3}{\chi^3 + c_{v1}^3}, \quad \chi = \frac{\tilde{\nu}}{\nu}, \quad \nu = \frac{\mu_{dyn}}{\rho}, \quad \tilde{S} = S + \frac{\tilde{\nu}}{\kappa^2 d^2} f_{v2}, \\ f_{v2} = 1 - \frac{\chi}{1 + \chi f_{v1}} \quad f_w = g \left[\frac{1 + c_{w3}^6}{g^6 + c_{w3}^6} \right]^{1/6}, \\ g = r + c_{w2}(r^6 - r), \quad r = \min \left(\frac{\tilde{\nu}}{\tilde{S} \kappa^2 d^2}, r_{max} \right) \end{aligned} \tag{4}$$

where S is the vorticity magnitude term computed as $S = |\nabla \times \mathbf{V}|$, and d is the distance to the nearest wall location. Parameters used in these equations are as follows:

$$\begin{aligned} \sigma = 2/3,\ c_{b1} = 0.1355,\ c_{b2} = 0.622,\ \kappa = 0.41,\ c_{w1} = \frac{c_{b1}}{\kappa^2} + \frac{1 + c_{b2}}{\sigma}, \\ c_{w2} = 0.3,\ c_{w3} = 2,\ c_{v1} = 7.1,\ r_{max} = 10 \end{aligned} \tag{5}$$

A modification was introduced recently [Crivellini et al., 2013; Crivellini and DAlessandro, 2014] to cure the problem of negative $\tilde{\nu}$ values, through simply avoiding negative valued computations and accompanying numerical difficulties. The source term, $\Pi - \Phi$, of the convection equation was rearranged and redefined as,

$$\Pi - \Phi = \begin{cases} \left[(1 - f_{t2}) \frac{c_{b1}}{\kappa^2 r} - c_{w1} f_w + f_{t2} \frac{c_{b1}}{\kappa^2} \right] \left(\frac{\tilde{\nu}}{d_w} \right)^2 + \frac{c_{b2}}{\sigma} |\nabla \tilde{\nu}|^2 & \tilde{\nu} \geq 0 \\ 0 & \tilde{\nu} < 0, \end{cases} \tag{6}$$

and the diffusion term was modified to be

$$\Psi = \nabla \cdot \left(\frac{\nu + \max[\tilde{\nu}, 0]}{\sigma} \nabla \tilde{\nu} \right) \tag{7}$$

In addition, the function r was redefined as

$$r^* = \left(\frac{S \kappa^2 d_w^2}{\tilde{\nu}} + f_{v2} \right)^{-1} \tag{8a}$$

$$r = \begin{cases} r_{max} & r^* < 0 \\ \min(r^*, r_{max}) & r^* \geq 0 \end{cases} \tag{8b}$$

Last but not the least, evaluation of turbulent viscosity was limited to positive values as well,

$$\mu_{turb} = \rho f_{v1} \max(\tilde{\nu}, 0), \tag{9}$$

all the remaining functions and constants being kept as they are. Note also that the laminar suppression term f_{t2} is ignored.

It was reported that this modification had an apparent transition behavior, essentially in case of flows with laminar separation. For attached flows, however, transition must be induced in other ways.

Shear-Layer-Adapted Length Scale for the DDES (SLADDES): In the present solver a recently proposed remedy by [Shur et al., 2015] to delay of transition from RANS to LES mode is implemented as well. It consists of redefinition of the length scale that not only depends on the grid but also on the flow, and its three-dimensionality. Firstly, a vorticity dependent length scale is defined:

$$\tilde{\Delta}_\omega = \frac{1}{\sqrt{3}} \max_{n,m=1,8} |\mathbf{I_n} - \mathbf{I_m}| \tag{10}$$

where $\mathbf{I_n} = \mathbf{n}_\omega \times \mathbf{r_n}$, and $\mathbf{n}_\omega$ is the unit vorticity vector, while $\mathbf{r_n}$ is the position vector for the vertices of the cell ($n = 1, ..8$ for hexahedral cells). This formulation removes dependency of subgrid viscosity on cell length (mostly $\Delta_{max} = \Delta z$ for a shear-layer in xy plane) in vorticity direction, which had been a problem in shear-layers where the planar shear is expected to initiate transition to the LES mode. Instead, the subgrid viscosity is based on the maximum dimension on the shear plane in a quasi-2D region. Still, the resulting reduction of the subgrid viscosity is not sufficient to initiate the transition in quasi-2D regions. An ILES(improved large-eddy simulation)-like behavior is desired in such regions to allow Kelvin-Helmholtz (K-H) instabilities to take over. The so-called "Vortex Tilting Measure" (VTM) is defined to detect such regions,

$$VTM = \frac{\sqrt{6}|(\hat{\mathbf{S}} \cdot \omega) \times \omega|}{\omega^2 \sqrt{3tr(\hat{\mathbf{S}}^2) - \left[tr(\hat{\mathbf{S}})\right]^2}} \tag{11}$$

It yields zero when the vorticity is aligned with any eigenvectors of the strain; nonzero when the deformation tensor tilts the vorticity vector. VTM is facilitated in the function

$$F_{KH}(\langle VTM \rangle) = \max\left[F_{KH}^{min}, \min\left\{F_{KH}^{max}, F_{KH}^{min} + \frac{F_{KH}^{max} - F_{KH}^{min}}{a_2 - a_1}(\langle VTM \rangle - a_1)\right\}\right] \tag{12}$$

where the angle brackets, $\langle \cdot \rangle$, means the value is averaged among neighboring cells. Averaging is necessary for smoothing the distribution since it is reported that VTM may have downward excursions locally. F_{KH} function is a simplistic function depending on VTM with the sole purpose of reducing the subgrid viscosity properly. $F_{KH}^{max} = 1$ recovers the original length scale while $F_{KH}^{min} = 0.1$, and $a_1 = 0.15$, $a_2 = 0.3$ are constants adjusted through numerical experiments. Accordingly, F_{KH} varies linearly between $\langle VTM \rangle = 0.15$ and $\langle VTM \rangle = 0.3$ yielding values ranging from 0.1 to 1. Hence, the ultimate subgrid length scale is calculated by

$$\Delta_{SLA} = \tilde{\Delta}_\omega F_{KH}(\langle VTM \rangle) \tag{13}$$

The resulting length scale serves as a reduction to the vorticity-oriented length scale, $\tilde{\Delta}_\omega$, up to one order in regions where K-H instabilities are expected to occur, thus leaving ground to transition to resolved 3D turbulent mode. However, for wall bounded flows, this reduction should be inactivated to keep the boundary layer shielded as done in standard DDES with Δ_{max}. The following limitation to F_{KH} was proposed for that purpose,

$$F_{KH}^{lim} = \begin{cases} 1.0 & f_d < 0.99 \\ F_{KH} & f_d \geq 0.99 \end{cases} \tag{14}$$

As a result, this version of DDES has proven success (by [Shur et al., 2015]) not only in free shear-layers, but also in wall bounded flows, jet flows, decaying turbulence, and backward facing step flows which is very similar to separation of the shear-layer from the front edge of the cavity of this study, which is described in the subsequent section.

Problem Definition

An unsteady, 3D, transonic flow over a typical open cavity geometry is simulated via SLADDES approach. The length-to-depth ratio (L/D), and the length-to-width ratio (L/W) of the cavity are both taken as 5. Simulations are done with a Reynolds number of 6.75×10^6, and Mach number of 0.85.

The Computational Domain:

The structured computational domain constructed for the computations is shown in Figure 1. The multiblock mesh domain is composed of two blocks. The first block, which represents the inside of the cavity, has $720,981$ grid points. There are 5 wall surfaces inside of it. The upper surface of this block is a fluid interface shared with the second block. On the other hand, the second block has $2,004,033$ grid points and it forms the outside of the cavity. The mesh is created in compliance with expectations of the RANS mode near the walls, LES region from RANS region to Euler region where the turbulent structures are almost dissipated, and Euler region from LES to the far field boundaries. The LES region has mostly isotropic cells which also includes the turbulent structures bounced after the impingement on the aft wall. Note that the computational domain of the IDDES and the LES studies had nearly 28 million and 12 million cells, respectively. Consequently, the current study has a very coarse mesh domain when compared with these benchmark studies.

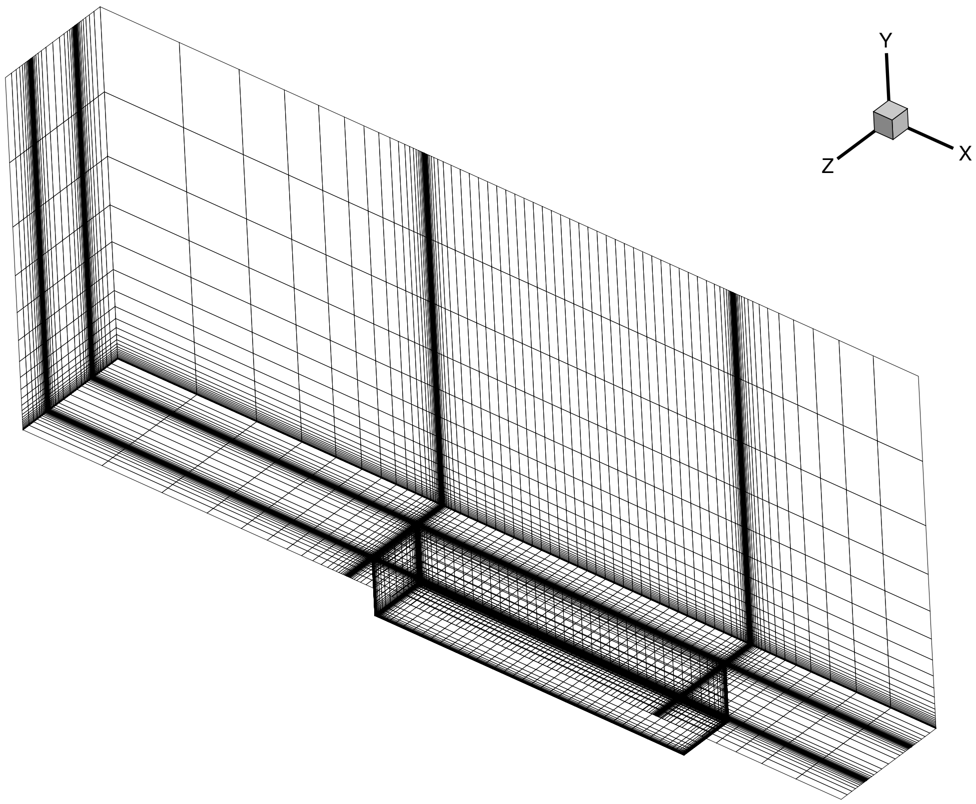

Figure 1: The multiblock structured mesh domain shown with only odd-numbered grids at IJK plane surfaces around an open cavity geometry with $L/D = 5$.

Boundary Conditions

At the upstream farfield, the free stream velocity and pressure are supplied with use of Riemann invariants whereas pressure outlet condition is applied at the downstream and the upside farfield. In the spanwise direction periodic boundary condition is applied. At the wall boundaries no-slip condition is enforced. To capture the inflow velocity profile, symmetry condition is enforced as long as the half of the cavity length until the wall boundary of the second block starts.

RESULTS AND DISCUSSION

Simulations are carried on until the flow statistics are converged. Convergence required approximately 5 cavity length convection times base on the free-stream velocity. Parallel computations are done with 64 processors.

The computed mean streamwise velocity profiles, and turbulent kinetic energy values at three stations in the flow field are drawn in Figure 2. The first station represents the points just after the leading edge ($x/D = 0.003$) whereas the second one represents at the middle of the length ($x/D = 2.5$) and the last one represents just before the trailing edge ($x/D = 4.997$) of the cavity. The points at all stations locates starting from the cavity floor to the outside the cavity ($y/D = -1.0$ to 1.0) at the central plane ($z/D = 0.5$). $y = 0$ line identifies the cavity mouth along the shear-layer. Both horizontal axes are scaled for better plotting. Both of the results at the first station show that DDES with shear-layer-adapted length scale captures the separated shear-layer profile just as the LES study. IDDES study with standard length scale, however, shows a profile like laminar flow unlike the other studies. Through the aft wall of the cavity, IDDES obtains closer results to LES than SLADDES. The reason of better capturing the flow phenomena around the aft wall in IDDES study might be the activation of the wall-modeled LES mode thanks to the much finer mesh when compared with the SLADDES study.

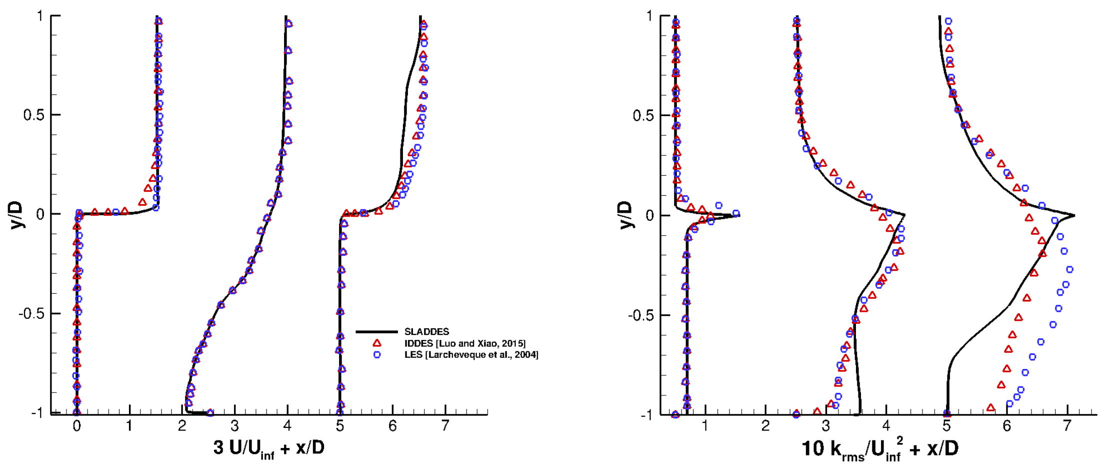

(a) Mean streamwise velocity profiles at $x/D = 0.003, 2.5$, and 4.997 stations

(b) Turbulent kinetic energy at $x/D = 0.5, 2.5$, and 4.5 stations

Figure 2: Comparisons of different flow profiles at three stations at the central plane. Horizontal axes are scaled for better plot.

Figure 3 shows the Mach number contour and the streamlines of the mean flowfield at the central plane. As seen in this figure, the streamlines go along the cavity mouth without significant variations. This is a typical behavior of the open cavity flow as mentioned in the "Introduction" section. Inside the cavity, two secondary flows (large and small vortices) are observed. Large vortices appear to span the entire cavity. Small vortices seem to exit only around the aft wall. According to the benchmark studies, the large one should be wider through the aft wall so that the upstream part of the streamlines would not bend so much as in Figure 3. This could be the reason why the deflections occur around the trailing edge.

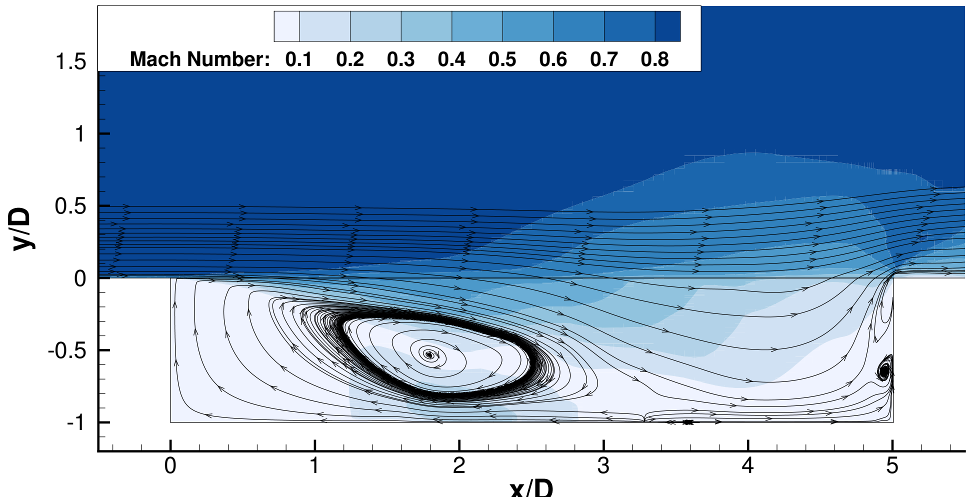

Figure 3: Mach number contour and the streamlines at the central plane for the mean flow.

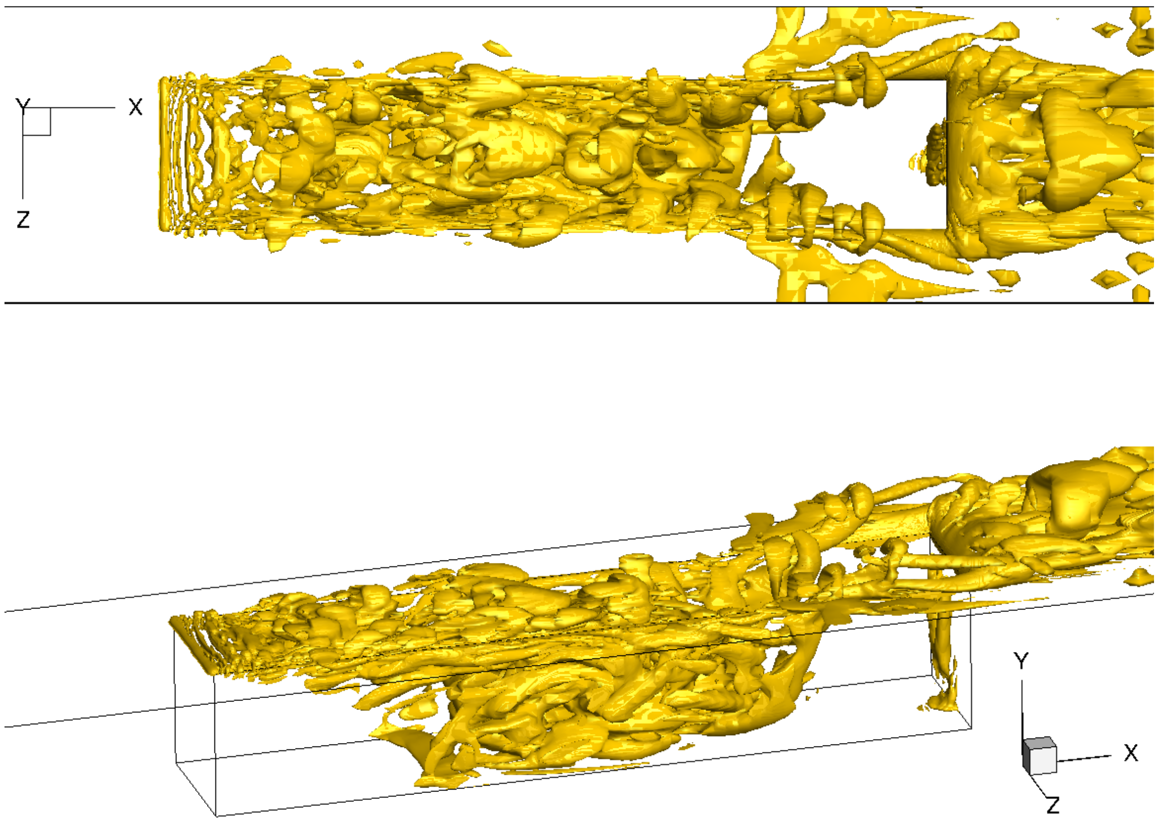

Figure 4: Iso-surfaces of Q-criterion (Q$= 100,000$) around the cavity domain from different views.

Iso-surfaces from the Q-criterion are shown in Figure 4. Q-criterion helps to visualize the vortex core regions around the specified domain. The value is selected as $100,000$ for clear visualization of turbulent related vortices just around the cavity mouth. The top view of the iso-surfaces demonstrate that when shear-layer is separated from the leading edge, firstly the 2D vortical tubes are observed. Then, they suddenly turn into 3D structures as seen in Figure 4. When properly measured, the location of the first appearance of the 3D structures is $x/D \approx 0.15$. This point is the exact location of the end region of the K-H instabilities in the LES study. However, in the IDDES study, 3D turbulent vortices were observed around $x/D \approx 0.5$, which shows that the standard length scale in DDES approaches damps the K-H instabilities and behave as URANS instead.

CONCLUSIONS

In this paper a DDES study with the recent subgrid length scale enhancement, known as shear-layer-adapted DDES, around an open cavity geometry was carried out. A typical open cavity flow behavior except at the aft wall region was observed using SLADDES. While uniform streamlines occured along the shear-layer except around the aft corner, large and small vortices appeared inside the cavity as secondary flow. The results of the turbulent flow domain were compared also with those of an IDDES study using standard length scale [Luo and Xiao, 2015] and an LES study [Larchevêque et al., 2004]. The current and LES studies equally predicted the location of first appearance of 3D vortical structures along the shear-layer just after the leading edge of the cavity, whereas the IDDES study predicted this location a bit further downstream. It seemed the shear-layer-adapted length scale accelerated the transition from modeled to resolved mode of DDES. Hence, as expected SLADDES unlocked the K-H instability waves and the separation region could be captured as opposed to the IDDES study. The study demonstrated that the employed recent length scale performs better in regions where the gray-area problem of DES shows up. On the other hand, the IDDES study showed closer results to the LES study than the current study through the aft wall. SLADDES may have needed a finer mesh resolution around this region, preferably as fine as the IDDES study, or as a wall-modeling approach would have, probably.

ACKNOWLEDGEMENT

The authors are grateful to RÜZGEM (METU Center for Wind Energy) for providing the HPC resources.

References

Richard Allen, Fred Mendonça, and David Kirkham. Rans and des turbulence model predictions of noise on the m219 cavity at m= 0.85. *International Journal of Aeroacoustics*, 4(1):135–151, 2005.

Kenan Cengiz and Yusuf Özyörük. Detached eddy simulation using a high-order low-dissipation low-dispersion computational method for aeroacoustic purposes. In *Ankara International Aerospace Conference, METU Ankara Campus*, 2015.

Andrea Crivellini and Valerio DAlessandro. SpalartAllmaras model apparent transition and RANS simulations of laminar separation bubbles on airfoils. *International Journal of Heat and Fluid Flow*, 47:70–83, June 2014.

Andrea Crivellini, Valerio DAlessandro, and Francesco Bassi. A SpalartAllmaras turbulence model implementation in a discontinuous Galerkin solver for incompressible flows. *Journal of Computational Physics*, 241:388–415, May 2013.

X Gloerfelt, C Bailly, and D Juvé. Direct computation of the noise radiated by a subsonic cavity flow and application of integral methods. *Journal of Sound and Vibration*, 266(1):119–146, 2003.

Awatef Hamed, D Basu, and K Das. Detached eddy simulations of supersonic flow over cavity. *AIAA paper*, 549:2003, 2003.

Duk Hyun Kim, Jae Hoon Choi, and Oh Joon Kwon. Detached eddy simulation of weapons bay flows and store separation. *Computers & Fluids*, 121:1–10, 2015.

J.C. Kok. A high-order low-dispersion symmetry-preserving finite-volume method for compressible flow on curvilinear grids. *Journal of Computational Physics*, 228(18):6811–6832, October 2009.

Huanxin Lai and Kai H Luo. A three-dimensional hybrid les-acoustic analogy method for predicting open-cavity noise. *Flow, turbulence and Combustion*, 79(1):55–82, 2007.

Lionel Larchevêque, Pierre Sagaut, Thien-Hiep Le, and Pierre Comte. Large-eddy simulation of a compressible flow in a three-dimensional open cavity at high reynolds number. *Journal of Fluid Mechanics*, 516:265–301, 2004.

SJ Lawson and GN Barakos. Review of numerical simulations for high-speed, turbulent cavity flows. *Progress in Aerospace Sciences*, 47(3):186–216, 2011.

Kunyu Luo and Zhixiang Xiao. Improved delayed detached-eddy simulation of transonic and supersonic cavity flows. In *Progress in Hybrid RANS-LES Modelling*, pages 163–174. Springer, 2015.

P Nayyar, GN Barakos, and KJ Badcock. Analysis and control of weapon bay flows. In *NATO RTO AVT-123 Symposium on Flow Induced Unsteady Loads and the Impact on Military Applications, Budapest*, pages 24–28, 2005.

Mark A Potsdam, Venkateswaran Sankaran, and Shishir A Pandya. Unsteady low mach preconditioning with application to rotorcraft flows. In *Proceedings of the 18th AIAA CFD Conference, Miami, FL*, 2007.

D Rockwell and Et Naudascher. Reviewself-sustaining oscillations of flow past cavities. *Journal of Fluids Engineering*, 100(2):152–165, 1978.

JE Rossiter. Wind tunnel experiments on the flow over rectangular cavities at subsonic and transonic speeds. Technical report, Ministry of Aviation; Royal Aircraft Establishment; RAE Farnborough, 1964.

Mikhail L Shur, Philippe R Spalart, Mikhail Kh Strelets, and Andrey K Travin. An enhanced version of des with rapid transition from rans to les in separated flows. *Flow, Turbulence and Combustion*, 95(4):709–737, 2015.

P Spalart and S Allmaras. A one-equation turbulence model for aerodynamic flows. In *30th Aerospace Sciences Meeting and Exhibit*, Aerospace Sciences Meetings. American Institute of Aeronautics and Astronautics, January 1992.

E. Turkel. Preconditioning-squared methods for multidimensional aerodynamics. In *13th Computational Fluid Dynamics Conference*, Snowmass Village, CO, U.S.A., jun 1997. American Institute of Aeronautics and Astronautics. URL `http://dx.doi.org/10.2514/6.1997-2025`.

Eli Turkel and Veer N Vatsa. Local preconditioners for steady and unsteady flow applications. *ESAIM: Mathematical Modelling and Numerical Analysis*, 39(03):515–535, 2005.